Noncoherent Frequency Shift Keying for Ambient Backscatter over OFDM Signals Using ANN

Shamli Dubey
M.Tech Scholar, Department of Electronics and Communication Engineering, Kanpur Institute of Technology, Kanpur, India.

Dr. Sweta Tripathi
Assistant Professor, Department of Electronics and Communication Engineering, Kanpur Institute of Technology, Kanpur, India.

Abstract:

In this research, we study the use of binary frequency shift keying (BFSK) over ambient OFDM signals to achieve higher performance. BFSK may be implemented by cycling through a succession of antenna loads that each provide a distinct phase shift at the tag. This allows us to unidirectionally shift the ambient spectrum either up or down in frequency, which allows us to implement BFSK. We take advantage of the guard band and the orthogonality of the OFDM subcarriers in order to avoid both direct-link and adjacent channel interfering signals. In contrast to energy detection-based approaches, which suffer from asymmetric error probability, the suggested scheme has symmetric error probabilities, which makes it more reliable. The proposed Artificial Neural Networks model analyses all of the data in this model and provides conclusions. In addition, we investigate the error performance of the optimal noncoherent detector and derive an accurate formula for the average likelihood of error from the results of our investigation. Finally, simulation results support our findings, demonstrating that the suggested technique surpasses energy detection-based schemes already existing in the literature by up to 3 dB in terms of sensitivity.

Index Terms

Ambient backscatter, internet of things, green communications, performance analysis, OFDM.

1. INTRODUCTION

It is expected that the Internet of Things (IoT) will fundamentally alter human-to-human (H2H), human-to-device (H2D), and machine-to machine (M2M) interactions in the not too distant future. A wide range of intelligent pervasive applications in diverse sectors of human life, including as agriculture, transportation, commerce, and healthcare, will result as a result. The solution to the restricted energy challenge that IoT devices are experiencing is critical to enabling such applications. The use of ambient backscatter has recently gained popularity as a viable option for enabling low-power and long-term operation of Internet-of-Things devices.

The Internet of Things network (IoT) in the future is envisaged to contain countless devices, many of which will be restricted severely in terms of price and energy consumption. In order to accomplish this perception, newly energy-efficient and low-cost communication mechanisms must be developed and implemented. Backscatter radio is one of the most promising technologies for meeting the escalating connection is in high demand. In typical ultra-low power equipments, backscatter radio systems, tags, which are commonly referred to as labels, have the ability to communicate. by simply connecting their antenna to various loads in order for reflecting and phaseshift encroaching RF signals a device for reading, which is then able to communicate with them. As a result, all signal processing that consumes a lot of power is contained in the reader, enabling for ultra-low-power tagging to be implemented without the use of several power-hungry RF components that are active, such as power amplifiers and ADCs, which would otherwise be required. Traditional backscatter radio systems, such as RFID, on the other hand, necessitate the construction of a dedicated infrastructure in order to deliver clean steady tags' illumination to transmit. A proposal in [1] suggests that backscatter tags be illuminated using current ambient RF transmission from standard cellular networks, TV, and WiFi rather of dedicated equipment, thus alleviating the requirement for dedicated infrastructure. As long as We have the ability to piggyback information on top of ambient radio frequency signals, we will be able to achieve ultra-low-power radio communications are prevalent, since RF broadcasts are ubiquitous. The utilization of previously modulated RF signals for backscatter, on the other hand, presents a number of difficulties.

Various smart signaling strategies for ambient backscatter were developed in recent years, and many of these systems are still under development. [1–5] demonstrated that ambient backscatter is a feasible technology through their early prototypes. In [1,] ambient television transmissions were used to develop a link amongst two batteries-free tags, which was previously unattainable. A simplistic averaging detector was employed to decode the values of tag because the signal backscatters at a considerably lower than that of a high-bandwidth television signal utilized in the experiment. It has been demonstrated in [2] that higher bit-rates and greater communication ranges can be acquired by reducing direct interference originating from the environment and employing signalling with a more robust transverse spread spectrum. When a tag and a commercial off-the-shelf WiFi device communicate bidirectionally via WiFi, equipment was shown [3]. Receiving signal strength (RSSI) indicator readings in uplink, as well as energy detection of brief WiFi packets in downlink, have enabled this to be accomplished. A WiFi AP with full-duplex capability has been

utilized in [4] to enable coherent phaseshift keying, which is capable of cancelling interfering with direct links and estimating channel. When moved to two neighboring channels utilizing fast On-off Keying (OOK), Bluetooth and WiFi signals are received utilizing commodity radios, as shown in [5,]. Furthermore, it has been demonstrated in[6]–[8] that backscatter may be used to produce packets for different standards. As demonstrated in [6, it is possible to produce WiFi packets Modified Bluetooth packets are backscattered. While FM signals as well as LoRa signals were formed by backscattering ambient signals with almost the same modulation in [7, 8], accordingly, FM signals and LoRa signals were generated by backscattering ambience signals with the very same modulation in [7, 8], respectively.

Because of early prototypes that look promising, a flurry of study was conducted to investigate even more hypothetical elements of ambient backscatter, like modeling, error efficiency, and capacity analysis [9, 14, 15]. It was demonstrated in [9] that the addition of nodes with a backscattering effect to a historical MIMO communication system enhances the maximum sum-rate that is attainable. According to [10] and [11], the differential encoding as well as averaging detection system's performance, which was first presented in [1,] was evaluated for the reader in the consists of a single antenna and for the case of multiple antennas. In [12] and [13], you can find additional study on the detection performance of ambient backscatter that is either noncoherent or semicoherent in nature. Earlier research makes no assumptions about the modulation of the source ambiant and depends mainly on Gaussian assumptions to approximate the modulation.

Gaussian approximations are used in this case. Since the majority of existing orthogonal frequency division multiplexing is used in wireless networks (OFDM), several researchers have attempted to utilize the OFDM waveform's structure in order to create more robust communications against ambient backscatter noise. Using remaining portion of the cyclic prefix, [14] was shown to be effective in cancelling interference of direct-link. However, in [15], orthogonality of OFDM subcarriers was leveraged in order to prevent interfering with direct links by transferring energy backscattered to nullify subcarriers, hence avoiding direct link interference. The two techniques stated above are based on energy detection and suffering from asymmetric error performance as well as laborious threshold computation procedures. Eventually, it was demonstrated in [16] that ambient backscatter could be used to the advantage of historical Transmissions using OFDM by providing a type of diversity in the transmission.

In this study, We look into binary frequency shift keying a background of OFDM signals using an experimental setup. The following are some of the main points of our contributions in this paper:

• Backscattering modulation over ambient OFDM carriers is proposed as a mechanism for enabling binary frequency shift keying modulation. The proposed frequency shifting technique differs from those other frequency shifting methods in that it depends upon cycling through into backscattered energy to neighboring channels on both sides of an ambient signal due to phase shifts of a complicated sinusoid. This allows for frequency shift in one direction without introducing sidebands or other unwanted frequency harmonics into the signal.

• We investigate the most efficient noncoherent detector and derive a precise equation for the average likelihood of mistake in the process. Instead of relying on energy detection as in previous schemes [14, 15], our ideal detector has symmetric error probability for both "0"s

and "1," as well as the ability to operate without needing to estimate an SNR- reliant threshold.

• This paper presents simulation data to support our assessment and to investigate the influence of system characteristics, such as the distribution of the maximum channel delay and the size of an OFDM symbol, on error performance. According to our findings, the suggested technique outperforms systems based on energy sensing in [14] and [15], respectively.

2. LITERATURE REVIEW

F. Jameel, W. U. Khan [17] ambient backscatter communication (AmBC) has emerged as a viable paradigm for enabling the long-term operation of Internet of Things (IoT) devices with minimal power consumption. Due to its capability of enabling sensing and communication through the use of backscattering ambient wireless signals, it is becoming increasingly popular (such as: WiFi and TV signals). However, one significant hurdle to the deployment of AmBC-enabled networks is the difficulties in decoding the backscatter signals because the ambient signals are typically encoded and intended for other legacy receivers rather than AmBC devices. The capacity of machine learning (ML) to improve the performance of wireless communication systems has inspired the development of various ML-aided techniques to aid signal recognition in acoustic-based communication systems (AmBC). In order to provide a comprehensive overview of the subject, this paper includes sections on: describing the operation of the AmBC network, highlighting the major challenges to signal detection in AmBC, discussing and comparing the performance of some existing ML-assisted solutions to AmBC signal detection, and outlining some future research that could be conducted on the subject.

Matsuoka, H.; Doi, Y.; Yabe, T.; Sanada, Y. [18] In this paper, the performance of a repetition coded overloaded multiple-input multiple-output (MIMO) orthogonal frequency division multiplexing (OFDM) system with multiple outputs is discussed. Signal multiplexing causes performance degradation, and it has been proved that diversity combined with block coding prevents this degradation from occurring. Despite this, the computing complexity of a joint decoding approach increases exponentially with the number of multiplexed signal streams that must be processed. As a result, the usage of a repetition code in an overloaded MIMO-OFDM system is proposed in this study effort. To further improve decoding performance, the QR decomposition with M-algorithm (QRM) maximum likelihood decoding (MLD) method is used to decode the repeating code. QRM-MLD considerably minimises the amount of complexity associated with joint decoding. In addition, virtual antennas are used to boost the throughput, which has been reduced as a result of the use of the repetition code. On the basis of six signal streams using QPSK modulation, it is discovered that the suggested system decreases complexity by approximately 1/48 while maintaining BER deterioration of less than 0.ldB at the BER of 10-3.

Long Shi; Wei Zhang; Xiang-Gen Xia, [19] the subject matter was investigated For multiple-input multiple-output (MIMO) wireless communications, partial interference

cancellation group decoding is a viable decoding option that offers a number of advantages. When it comes to space-time block codes, it is well suited for dealing with the tradeoff between rate, diversity, and decoding difficulty. It is proposed in this study effort to use a full-diversity space-frequency code (SFC) as a design criterion for MIMO-OFDM systems with PIC group decoding in order to achieve high performance. Following this condition, a systematic design of full-diversity SFC is proposed. This design is capable of achieving full diversity under the PIC group decoding scheme. The simulation results of the recently proposed codes indicate the validity of the hypothesis in question.

Doi, Y.; Inamori, M.; Sanada, Y., [20] In an overloaded multiple-input multiple-output (MIMO) orthogonal frequency division multiplexing (OFDM) system, a low-complexity joint decoding approach for block coded signals was presented. An evaluation of a joint maximum likelihood decoding technique for block coded signals has been done previously in the literature using theoretical analysis. The diversity increase achieved through block coding avoids the performance decrease caused by signal multiplexing from becoming apparent. The computational cost of the joint decoding approach, on the other hand, increases exponentially with the number of multiplexed signal streams that are decoded simultaneously. This study suggests a two-step collaborative decoding approach for block coded signals, which is described in detail elsewhere. To begin, the suggested approach produces metrics to lower the number of candidate codewords employing decoding based on joint maximum like hood symbol detection in order to reduce the number of candidate codewords. The joint decoding of the reduced candidate code words is performed in the second process of the suggested scheme in the third step.

3. SYSTEM MODEL

Figure 1 depicts a classical three-node ambient backscatter system model, which is discussed further in [14], [15], and [21]. A common assumption in the field of ambient backscatter communications is that there is a typical communication system that already exists, which will be alluded to such as the archaic communications system that generates RF signals. We will assume that the historical communication system is based on OFDM, such as WiFi or LTE. The archaic communication nodes are equipped with classic active transceivers that are supplied by massive capacity batteries or are linked to the power grid, and as a result, they are undeterred by the weaker backscattered signals that are transmitted. A different type of communication system, known as surreal backscatter communication, is comprised of tags that communicate using ultra-low power by varying respective antenna capacities in order to reflect signals from the ambient to the receiver. The tags could only be powered by energy harvested from the environment, whilst the reader is a regular radio transceiver with a battery backup.

Consider that there is a single one tag, one reader and ambient source, with just a single antenna each, and that every channel is a multipath channel that is uncorrelated channels for Rayleigh fading with no overlap in signal strength. To signify the impulse responses of channel amongst ambient source and receiver, amongst ambient source and the tags, and

amongst tag and receiver, let g (t), h (t), and f (t) be denoted by the letters G (t), H (t), and F (t). The related delay spreads are shown as by τf, τh and τg.

The bandpass signal generated by the legacy transmitter has the following representation

$$s(t) = \Re\left\{\sqrt{\rho}\; s_l(t)\, e^{j2\pi f_c t}\right\}, \qquad (1)$$

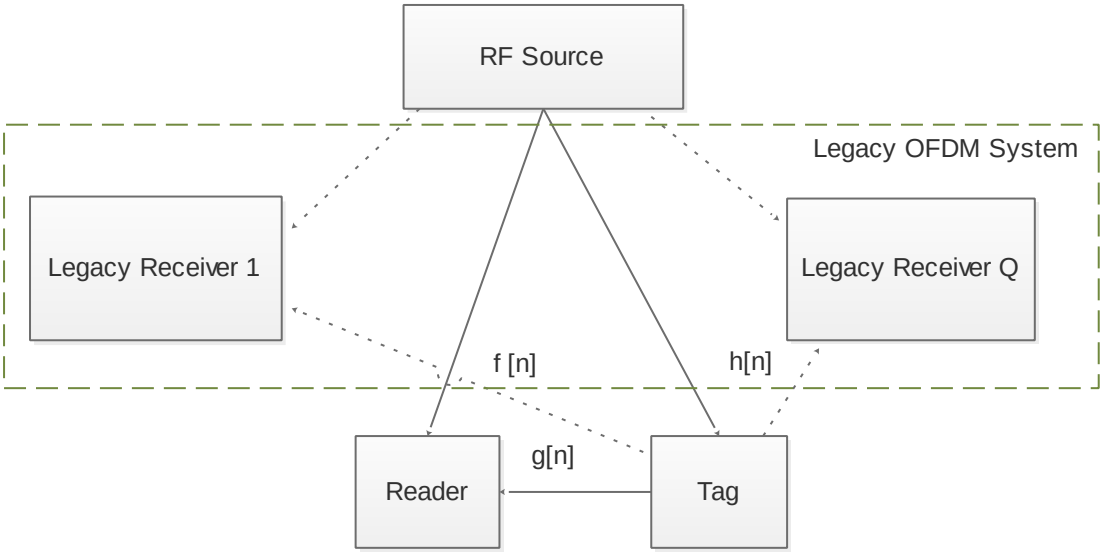

Figure 1: System Model

where$\Re\{\cdot\}$ represents real-part operator, $s_l(t)$ is the baseband representation of $s(t)$, ρ is average transmitted power, and fc is center frequency. Therefore, signal received at tag is represented by

$$x(t) = \Re\left\{\left[\sqrt{\rho}\; s_l(t) * h_l(t)\right] e^{j2\pi f_c t}\right\}, \qquad (2)$$

Where $*$ represents linear convolution, and $x_l(t) = \sqrt{\rho} s_l(t) * h_l(t)$ is baseband illustration of $x(t)$.

By linking its antenna to changing loads, the tag modulates the information. Hence, no thermal noise is restored at the tag [10,11,14]. Let $b_l(t)$ represents the modulation waveform of the tag's baseband representation with corresponding bandpass signal $b(t)$ and α represents coefficient of tag reflection. The signal received by the reader could be expressed as

$$y(t) = \underbrace{[\alpha x(t)\, b(t)] * g(t)}_{y^b(t)} + \underbrace{s(t) * f(t)}_{y^d(t)} + w(t), \qquad (3)$$

where $y^b(t) = [\alpha x(t)\, b(t)] * g(t)$ is signal backscatteredfrom the tag, $y^d(t) = s(t) * f(t)$ is direct signal from the vintage transmitter, and $w(t)$ is bandpassGaussian noise, which is autonomous of both $yb(t)$ and$yd(t)$. It's worth noting that the tag's information is only included in the word.

$y^b(t)$, while $y^d(t)$ is the direct-link (i.e. legacy-transmitterto reader) interference. The received signal's baseband representation is expressed as

$$y_l(t) = y_l^b(t) + y_l^d(t) + w_l(t), \qquad (4)$$

where$y_l^b(t)$, $y_l^d(t)$, and $w_l(t)$ denote the baseband representations of $y^b(t)$, $y^d(t)$, and $w(t)$, approximately.

The receiving signal is down-converted to baseband then routed through with an ADC converter just at reader. Let N_f represents number of subcarriers, or fast Fourier transform (FFT) length, andN_{cp}denote the length of cyclic prefix. For one OFDM symbol, the resulting discrete-time baseband sequence could be expressed as

$$y_l[n] = y_l^b[n] + y_l^d[n] + w_l[n], \quad n = 1, 2, \ldots, N_f + N_{cp}, \tag{5}$$

where$w_l[n]$ is complex baseband additive white Gaussiannoise (AWGN) with zero-mean and variance σ_w^2 . Let $h_l[n]$,$f_l[n]$, and $g_l[n]$ denote the discrete-time baseband representation of $h(t)$, $f(t)$, and $g(t)$, respectively, whoselengths aregiven by $L_h = [\tau_h f_s]$, $Lf = [\tau_f f_s]$, and $Lg = [\tau_g f_s]$, where$f_s$is the sampling frequency. Let τ , max $\{\tau_f, \tau_h + \tau_g\}$denote the maximum channel delay spread; hence, L ,max $\{L_f, L_h + L_g - 1\}$ represents the maximum channel delay spread's discrete-time duration. Furthermore, the tag reader distance is typically minimal in practise, hence it is plausible to believe $L_g = 1$ [14]. Then, we may write $y_l^b[n] = g x_l[n]\, b_l[n]$ and$y_l^d[n] = \sqrt{ps_l}[n] * f_l[n]$. We utilise the discrete-time baseband model throughout the rest of the work and omit the subscript l for notational reasons.

Our aim is to develop the tag modulation in such a way that totally noncoherent detection of b[n] as from received signal y[n] is possible without understanding the broadcast OFDM symbol s[n], the essential channels h[n], f[n], and g, or indeed the average SNR.

4. DESIGN AND PERFORMANCE EVALUATION OF TRANSCEIVERS

In this subsection, we suggest a frequency shift keying modulation technique for backscatter communications beyond OFDM signals that are present in the surrounding environment. We explain the waveform of tag modulation and investigate the most suitable noncoherent detector. The error performance of the suggested method is also examined, and an analytical equation for average error probability is obtained.

4.1. Tag Waveform Design

Of the subcarriers in OFDM systems, a portion of them are left blank to function as the guard band and to comply with FCC spectrum restrictions. These subcarriers are located near the margins of the spectrum nonetheless within the channel bandwidth. These guard bands were recently recommended as a part of deploying alternatives for narrow band Internet of Things (NB-IoT) devices[22]. The total subcarriers will be determined by channel bandwidth as well as spacing between the subcarriers. The inband null subcarriers at the margins of a 10.0MHz LTE signal, for example, are 64 in number. The groups of upper guard subcarriers as well as lower guard subcarriers, correspondingly, are denoted by U and L, and the set of lower guard subcarriers. "Upper" denotes to subcarriers that are higher in frequency than the centre frequency, and "lower" denotes to subcarriers that are lower in frequency than the centre frequency. In reality, there will be an equal number of upper as well as lower subcarriers in both the upper and lower carriers. For this reason, we expect $|\mathcal{U}| = |\mathcal{L}| = N$, whereas the symbol for cardinality is represented by $|\bullet|$.

Our tag modulation signal takes benefit of the two guard band subcarriers as well as the To prevent direct-link interference, OFDM's inherent orthogonality is used while permitting for quite basic square-law detection that is not dependent on signal strength. This is accomplished by selectively shifting the backscattered signal spectrum to one of lower or upper guard bands using a tag modulation waveform to broadcast one bit of information to the receiving station. As a result, the detector only needs to compare energy levels in two bands in order to decipher tag information. Neither the transmitted OFDM symbol nor any of necessary channels, nor even a threshold that is based on SNR, are required for the detector's operation. Overlaying binary frequency-shift (BFSK) keying on top of ambient signal might be considered as an improvement on the previous approach. We suggest a straightforward method that assures that no backscatter energy is redistributed outside of channel bandwidth, as previously described.

Allow each backscatter symbol to last the same amount of time as one destiny OFDM symbol [14,16]. The tag transmits one information bit for every OFDM signal using the waveform shown in the accompanying figure,

$$b[n] \triangleq \begin{cases} \mathrm{e}^{i2\pi \frac{N}{N_f} n}, & B = 0, \\ \mathrm{e}^{-i2\pi \frac{N}{N_f} n}, & B = 1, \end{cases} \qquad (6)$$

Where $n = 1, 2, \ldots, N_f + N_{cp}$ and $B \in \{0, 1\}$ is the information bit being transmitted. The tag's antenna will be connected to various loads and will cycle through a given number of defined phase shifts (in one orientation) to send a '1'bit, whereas tag would cycle through the identical antenna loads but in reverse direction to transmit a '0' bit (order). This is a well-researched problem, which was first encountered in the development of phase shiftkeying in backscatter tags and has since been investigated further. It is possible to find an example of a development in the context of backscatter from the environment in [4]. By just cycling via phase shifts, we may create complicated sinusoids and unidirectionally move the frequency spectrum of the environmental signal up or down without having to do anything complicated. It should be noted that, in contrast to [5] and [24], the proposed technique allows for unidirectional frequency shifts with no introduction of mixing sidebands or undesired frequency components, and that all backscattered energy is maintained within channel bandwidth, preventing interference from adjacent channels.

The backscattered signal obtained by reader can be represented as follows

$$y^b[n] = \begin{cases} \alpha g\, x[n]\, \mathrm{e}^{i2\pi \frac{N}{N_f} n}, & B = 0, \\ \alpha g\, x[n]\, \mathrm{e}^{-i2\pi \frac{N}{N_f} n}, & B = 1. \end{cases} \qquad (7)$$

Taken from (7), the backscattered signal spectrum is written as follows

$$Y^b[m] = \begin{cases} \alpha g X[m] \circledast \delta[m - N] = \alpha g\, X[m - N], & B = 0, \\ \alpha g X[m] \circledast \delta[m + N] = \alpha g\, X[m + N], & B = 1, \end{cases} \qquad (6)$$

Where $\circledast$ represents circular convolution, as well as Discrete Fourier Transform (DFT) of $x[n]$ is $X[m]$. Hence, from frequency domain viewpoint, to transmit a '0' bit, thetag shifts the

spectrum of backscattered signal into the upper guardband, $\mathcal{U}$, while to transmit a '1', tag shifts spectrum of the backscattered signal into the lower guardband,$\mathcal{L}$.

Where $\circledast$ signifies circular convolution and *X [m]* denotes the discrete Fourier transform (DFT) of the input signal *x [n]*. Accordingly, from the standpoint of the frequency domain, to transmit a "0" bit, thetag shifts the spectral range of backscattered signal into (*U*) upper guardband, while to transmit a "1," tag shifts spectral range of backscattered signal into (*L*) lower guardband. The tag shifts backscattered signal spectrum into both upper guardband, $\mathcal{U}$, and lower guardband, $\mathcal{L}$.

4.2. Detector

For practical purposes, the ambient backscatter receiver will not be able to distinguish between the ambient signal (OFDM), *s[n]*, and any of related channels, *h[n]*, *f [n]*, or *g*. As a result, we'll have to alter to noncoherent detection to get by. [25] Under situation of noncoherent FSK, square-law detector is certainly considered to be the most efficient. This detector, in contrast to the energy detection-dependent systems described in [14,15], doesn't depend on threshold and doesn't require the estimation of average SNR. The suggested detector necessitates that receiver only be aware of set of upper and lower guard subcarriers in order to function. Also demonstrated will be that it's symmetric error probability for both "0"s and "1"s, which is a significant benefit over energy detection-dependent techniques in terms of accuracy.

Consider the FFT output at the receiver, where *Y [m]* signifies the value of the output. Perhaps we may produce two statistical tests, one for upper guard band, $\mathcal{U}$, and one for the lower guard band, *L*.

$$E_u = \frac{2}{\sigma_w^2} \sum_{m \in \mathcal{U}} |Y[m]|^2, \qquad (9)$$

As well as one for the lower guardband, letter $\mathcal{L}$,.

$$E_l = \frac{2}{\sigma_w^2} \sum_{m \in \mathcal{L}} |Y[m]|^2. \qquad (10)$$

Depending on the outcomes of the tests, we can design our detection rule as follows

$$\hat{B} = \begin{cases} 0, & E_u > E_l, \\ 1, & E_l \geq E_u. \end{cases} \qquad (11)$$

$E_u$nor $E_l$suffers from direct link interference because the direct link signal does not present just on the data subcarriers; hence, $E_u$nor $E_l$suffers from direct link interference. It is important to note that, depending on the transmitted bit, $E_u$and $E_l$may are dependent on randomly backscatter channels *h[n]* and g. Following that, we look at distribution of statistical tests as well as the received signal to noise ratio (SNR).

For simplicity, we will refer to $\mathcal{H}_0$ and $\mathcal{H}_1$ as assumptions that the transmitted bit is a value of "0" or a value of "1." We begin by considering $\mathcal{H}_0$, which is the assumption that the transmitted bit is a '0.' Backscattered signal spectrum is relocated into upper guardband subcarriers, $\mathcal{U}$,, and lower guardband subcarriers, $\mathcal{L}$, comprise only noise when the backscattered signal spectrum is now under $\mathcal{H}_0$. As a result, E_l is just summation of squares of N standard Gaussian random variables in a uniform distribution. As a result, $E_l|\mathcal{H}_0 \sim \mathcal{X}^2_{2N}$, where $\mathcal{X}^2_{2N}$ denotes the central chi-squared variate with $2N$ degrees of freedom. When it comes to Eu, the random backscatter channel plays a critical role. This is the formula for the instantaneously received signal to noise ratio (SNR) in the upper guard band.

$$\gamma_u = \frac{\rho|\alpha|^2|g|^2 \sum_{m\in\mathcal{U}}|H[m]|^2}{N\sigma_w^2}, \qquad (12)$$

Where the coefficients of fading channel are observed by subcarriers of upper guard band and $\{H[m]\}m\in\mathcal{U}$are the coefficients of fading channel observed by subcarriers of lower guard band. As a result, depending on the instant received SNR, $Eu|\mathcal{H}_0 \sim \mathcal{X}^2_{2N}(2N\gamma_u)$ where $\mathcal{X}^2_{2N}(2N\gamma_u)$ is the chi-squared distribution of noncentral with degrees of freedom 2N and noncentrality variable $2N\gamma_u$.

During $H1$, the spectrum of backscattered signal is moved to the subcarriers of lower guard band, L, and we find ourselves in a reciprocal scenario to that which we found ourselves in under $\mathcal{H}_0$. E_u is defined as the summation of squares of standard Gaussian random variables N and following the distribution of central chi-squared, which is $E_u|\mathcal{H}_1 \sim \mathcal{X}^2_{2N}$ in this case. When it comes to the lower guard band sub-carriers, E_l is dependent on the immediate received SNR, which could be expressed as

$$\gamma_l = \frac{\rho|\alpha|^2|g|^2 \sum_{m\in\mathcal{L}}|H[m]|^2}{N\sigma_w^2}, \qquad (13)$$

In this case, $\{H[m]\}m\in\mathcal{L}$are the coefficients of fading channel, which are observed by subcarriers of lower guard band. As a result, $E_l|\mathcal{H}_0 \sim \mathcal{X}^2_{2N}(2N\gamma_l)$ is conditional on the instantaneous received signal strength. It is worth noting that, because $\{H[m]\}m\in\mathcal{U}$and $\{H[m]\}m\in\mathcal{L}$are equally distributed, the instantaneously received SNRs in subcarriers of upper and lower guard, U and l, are also similarly distributed, as is the case with the upper and lower guard subcarriers. Henceforth, the immediate received SNR in either band will be denoted by the symbol γ.

SNR γ is defined as the difference between two random variables: $|g|^2$ (an exponentially random parameter) and $q \triangleq \mathrm{P}_{m\in\mathcal{U}}|H[m]|^2$ (or identically $\mathrm{P}_{m\in\mathcal{L}}|H[m]|^2$) (which is summation of N associated exponential random variables), which is a scaling product of two random variables. In order for the subcarrier spacing to be less than the coherence bandwidth, there must be a correlation between these two parameters. h is the vector of channel coefficients

$\{H[m]\}_{m\in u}$ (or h is the vector of channel coefficients $\{H[m]\}_{m\in}$). Then, using the procedure outlined in [26], it is possible to determine that the distribution of q is

$$p(q) = \sum_{r=1}^{R} \left(\prod_{k\neq r} \frac{\frac{1}{\lambda_k}}{\frac{1}{\lambda_k} - \frac{1}{\lambda_r}} \right) \frac{1}{\lambda_r} e^{-\frac{q}{\lambda_r}}, \qquad (14)$$

In this case, the non-zero eigenvalues of such covariance matrix E [$\mathbf{hh}\dagger$] are represented by the $\{\lambda r\}^{R}_{r=1}$ symbol. With the help of the product distribution formula, it is possible to quickly determine the instant SNR distribution.

$$p(\gamma) = \sum_{r=1}^{R} \left(\prod_{k\neq r} \frac{\frac{1}{\lambda_k}}{\frac{1}{\lambda_k} - \frac{1}{\lambda_r}} \right) \frac{2N}{\lambda_r \overline{\gamma}} \mathbf{K}_0 \left(2\sqrt{\frac{N\,\gamma}{\lambda_r\,\overline{\gamma}}} \right), \quad (15)$$

The average detection SNR is given by $\triangleq E[\gamma] = |\alpha|^2\sigma/\rho^2_w$, and $\mathbf{K}m$ (·) is the modified Bessel function of the second type and m-th order is given by Km (•).

4.3. Error Performance

Following that, we look at the likelihood of an error in the proposed plan. Considering that the tag sent bits are equally likely to be ones or zeros, the chance of error can be calculated as follows:

$$P_e = \frac{1}{2}\left[P\left(\hat{B} = 1|\mathcal{H}_0\right) + P\left(\hat{B} = 0|\mathcal{H}_1\right)\right]. \qquad (16)$$

which is the same as saying

$$\begin{aligned} P_e &= \frac{1}{2}\left[P\left(E_l > E_u|\mathcal{H}_0\right) + P\left(E_u > E_l|\mathcal{H}_1\right)\right]. \\ &= \frac{1}{2}\left[P\left(\frac{E_l}{E_u} < 1|\mathcal{H}_0\right) + P\left(\frac{E_u}{E_l} < 1|\mathcal{H}_1\right)\right]. \end{aligned} \qquad (17)$$

Make a note of the fact that $E_l|\mathcal{H}_0 \overset{m}{=} E_u|\mathcal{H}_1$ and $El|\mathcal{H}_1 \overset{m}{=} E_u|\mathcal{H}_0$, where $\overset{m}{=}$ represents equivalence in distribution. As a result, we exhibit symmetric error probability under $\mathcal{H}_0$ and $\mathcal{H}_1$, in contrast to energy detection-dependent approaches [14, 15], which contain differing probability of false-alarm and missed-detection at ideal threshold, resulting in asymmetric detection probability.

Due to the fact that we would have symmetric error probabilities, it's adequate to determine error probability under the assumption $\mathcal{H}_0$. $E_l$and E_u in geographic distribution has already been covered in the preceding subsection. The chi-squared distribution of noncentral with noncentrality parameter $2N\gamma$ is followed by E_u, and the central chi-squared distribution with noncentrality parameter 2N is followed by Eu, both with 2N degrees of freedom, under H0 and conditional on channel. Being independent of one another El and Eu, the quotient $z \triangleq \frac{El}{Eu}$

follows the Fisher-Snedecorsingly noncentral *F*-distribution, whose probability density function can be represented by

$$p(z)=\sum_{j=0}^{\infty}\frac{e^{\delta/2}(\delta/2)}{B\left(\frac{v_2}{2},\frac{v_1}{2}+j\right)j!}\left(\frac{v_1}{v_2}\right)^{\frac{v_1}{2}+j}\left(\frac{v_2}{v_2+v_1z}\right)^{\frac{v_1+v_2}{2}+j}z^{\frac{v_1}{2}-1+j}, \quad (18)$$

Whereas B(•, •) denotes beta function, *v*1 and *v*2 denote the degrees of freedom of both the numerator and the denominator, correspondingly, and denotes the numerator noncentrality parameter, and the cumulative distribution function is denoted by the notation,

$$F(z;v_1,v_2,\delta)=\sum_{j=0}^{\infty}\left(\frac{\left(\frac{\delta}{2}\right)^j}{j!}e^{-\frac{\delta}{2}}\right)I\left(\frac{v_1z}{v_2+v_1z}|\frac{v_1}{2}+j,\frac{v_2}{2}\right) \quad (19)$$

In which *I* (*x*|*a*, *b*) is the incomplete beta function with parameters a and b. As a result, the likelihood of inaccuracy at any given time can be stated as

$$P_e=F(1;2N,2N,2N\gamma)=\sum_{j=0}^{\infty}\left(\frac{(N\gamma)^j}{j!}e^{-N\gamma}\right)I\left(\frac{1}{2}|N+j,N\right). \quad (20)$$

To calculate the average chance of mistake, multiply the error probability in [20] by the SNR distribution obtained in [15]. We may describe the average likelihood of error as by addressing the exponential and Bessel functionality in terms of Meijer G-function.

$$\overline{P_e}=\sum_{j=0}^{\infty}\sum_{r=0}^{R}\frac{N^j}{j!}I\left(\frac{1}{2}|N+j,N\right)\left(\prod_{k\neq r}\frac{\frac{1}{\lambda_k}}{\frac{1}{\lambda_k}-\frac{1}{\lambda_r}}\right)\times\int_0^{\infty}\gamma^{j-1}G_{0,1}^{1,0}\left(\overline{0}\,|\,N\gamma\right)G_{0,2}^{2,0}\left(\overline{1,1}\,\middle|\,\frac{N\,\gamma}{\lambda_r\,\overline{\gamma}}\right)d\gamma. \quad (21)$$

With the help of [27,07.34.21.0011.01], the integral in (21) may be solved to yield the final answer for the averaged error probability of error as

$$\overline{P_e}=\sum_{j=0}^{\infty}\sum_{r=0}^{R}\left(\prod_{k\neq r}\frac{\frac{1}{\lambda_k}}{\frac{1}{\lambda_k}-\frac{1}{\lambda_r}}\right)\frac{I\left(\frac{1}{2}|N+j,N\right)}{j!}\times G_{1,2}^{2,1}\left(\begin{matrix}1-j\\1,1\end{matrix}\,\middle|\,\frac{1}{\lambda_r\,\overline{\gamma}}\right). \quad (22)$$

In MATLAB, both incomplete beta function as well as Meijer G-function include built-in functions, enabling evaluation of this formula simple.

5. PROPOSED METHODOLOGY

An Artificial Neural Network (ANN) could be used to alter the weights and thresholds of a connectionist model by training datasets to map input and output variables. ANNs strive to get good results by connecting a large number of neurons together. An ANN model is identified by its architecture, which includes a sophisticated algorithm for training datasets. The network architecture defines the pattern of neuronal connections, whereas the activation function defines the type of unit. There are two modes of operation for the neural network: processing and training. Algorithms define how the neural units generate results for a certain set of inputs and weights in process mode. Algorithms define how the network adjusts its weights for all coaching patterns in coaching mode.

5.1 KNN CLASSIFIER

The kNN classifier, for example, is based on the assumption that the categorization of unknown instances is frequently done by linking the unknown to the familiar using some distance/similarity function. The intuition is that two instances that are so far apart in the instance space described by the appropriate distance function are less likely to belong to the same category than two instances that are close together. The goal of the k Nearest Neighbors (kNN) technique is to predict the categorization of fresh sample points using a database wherein the data points are segregated into many different classes.

McCulloch and Pitts [28] devised an artificial neuron structure that is similar to that of a biological neuron (F).

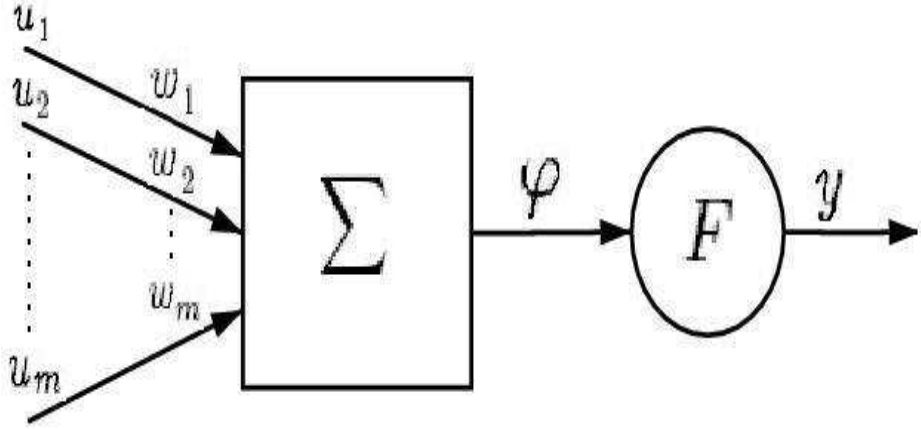

Figure.2 Mathematical Model of a single neuron [28].

There are two modules in it: the summation module Σ and the activation module F. The accumulation module is roughly equivalent to a biological nucleus. The output signal φ is formed by performing algebra summing of weighted input signals. The formula for calculating the output signal can be found here,

$$\varphi = \sum_{i=1}^{m} w_i u_i = w^T u \quad (23)$$

Where w is the weights vector (synapses comparable), u is the input signal vector (dendrites similar), and m is the number of inputs. The signal is handled by the activation module F that can be customized using various functions. The output signal y has form if a simple linear function is applied.

$$y = K \varphi \quad (24)$$

Networks that use this function are referred to as Madaline, and its neurons are referred to as Adaptive linear elements. They are the most basic networks that have found practical use. A threshold function is another sort of activation module function

$$f(x) = \begin{cases} 1, & \varphi > \varphi h \\ 0, & \varphi \leq \varphi h \end{cases} \quad (25)$$

A sigmoid function, on the other hand, describes a non-linear profile of a biological neuron more precisely when φh is a constant threshold value.

$$y = \frac{1}{1+ e^{-\beta\varphi}} \quad (26)$$

Where β is a tangensoid function and is a specified parameter

$$y = \tan h \left(\frac{\alpha\varphi}{2}\right)\frac{1- e^{-\alpha\beta}}{1+ e^{-\alpha\beta}} \quad (27)$$

Where α is the parameter that has been given. A single neuron's information capacity as well as processing ability is somewhat limited.

It can, however, be raised by the proper coupling of several neurons. Rosenblatt created the first artificial neural network, known as a perceptron, in 1958. It was used to recognise alphanumeric characters. Despite the fact that the findings were unsatisfactory, it was a success as the first system to simulate a neural network. Rosenblatt also shown that if a perceptron can solve a problem, the solution may be obtained in a finite number of steps. After nearly 15 years, research has been revived by a series of publications demonstrating that these constraints do not apply to non-linear multilayer networks. Learning strategies that are effective have also been introduced.

In multilayer ANNs, neurons are divided into three sorts of layers: input, output, and hidden layer. In a network, there can be one or more hidden layers, but only one output and one input layer. The type and amount of data that will be sent to the input determine the number of neurons in the input layer. The network's type of response is determined by the number of output neurons. It's more difficult to estimate the number of buried layers and their neurons. Most tasks can be solved with just one hidden layer in a network. In order to be solved, none of the known issues require a network with more than three hidden layers. Signals from the neurons in the input layer (IL) are routed to the hidden layer (HL), and then to the output layer (OL) (OL). There is no foolproof method for determining the number of hidden neurons. A formula is used to describe one of the methods.

$$N_h = \sqrt{N_i\, N_o} \quad (3.17)$$

Where N_i and N_o are the appropriate values for the input and output layers, correspondingly, and N_h his the number of neurons in the hidden layer. Therefore, the number of hidden neurons is normally chosen by trial and error.

6. RESULTS AND DISCUSSION

In this part, we use computer simulations to evaluate the proposed scheme's performance and to verify the analysis performed in Section 4. The OFDM system parameters by LTE standard are used in our simulation. The impact of maximum channel delay spread, and OFDM symbol size on error performance are investigated. Furthermore, we compare our suggested system to baseline energy detection-dependent approach from [15], which outperforms the other energy detection- dependent approach in [14].

The subcarriers of guard band along the margins of the spectrum of OFDM symbol are also used in [15].

To transmit a '1', tag's antenna impedance is switched amongst two states, causing spectrum of backscattered signal to fall on both sides of guard band.

When sending '0,' tag simply maintains impedance of its antenna. As a result, the tag information may be decoded using energy detection across the whole guard band. The threshold of energy detector will be a function of SNR, which will have to be determined at receiver; secondly, ML detector has asymmetrical error probability for '0's and'1's.

In Figure 3, we change the size of OFDM symbol, Nf, and compare proposed scheme's average bit-error rate to the baseline by [15] with perfect SNR calculation. For all OFDM symbol sizes, we find that proposed system outperforms the baseline. This is to be expected, given that noncoherent FSK is projected to outperform basic energy detection. Notably, the performance advantage appears to rise with SNR. For example, at a bit-error rate of 102, the suggested technique beats the baseline by roughly 2 dB, and at a BER of 103, the advantage climbs to more than 3 dB. We also notice that error probability calculated using analytical expressions, represented by markers, corresponds to simulation results, confirming our Section 4 analysis.

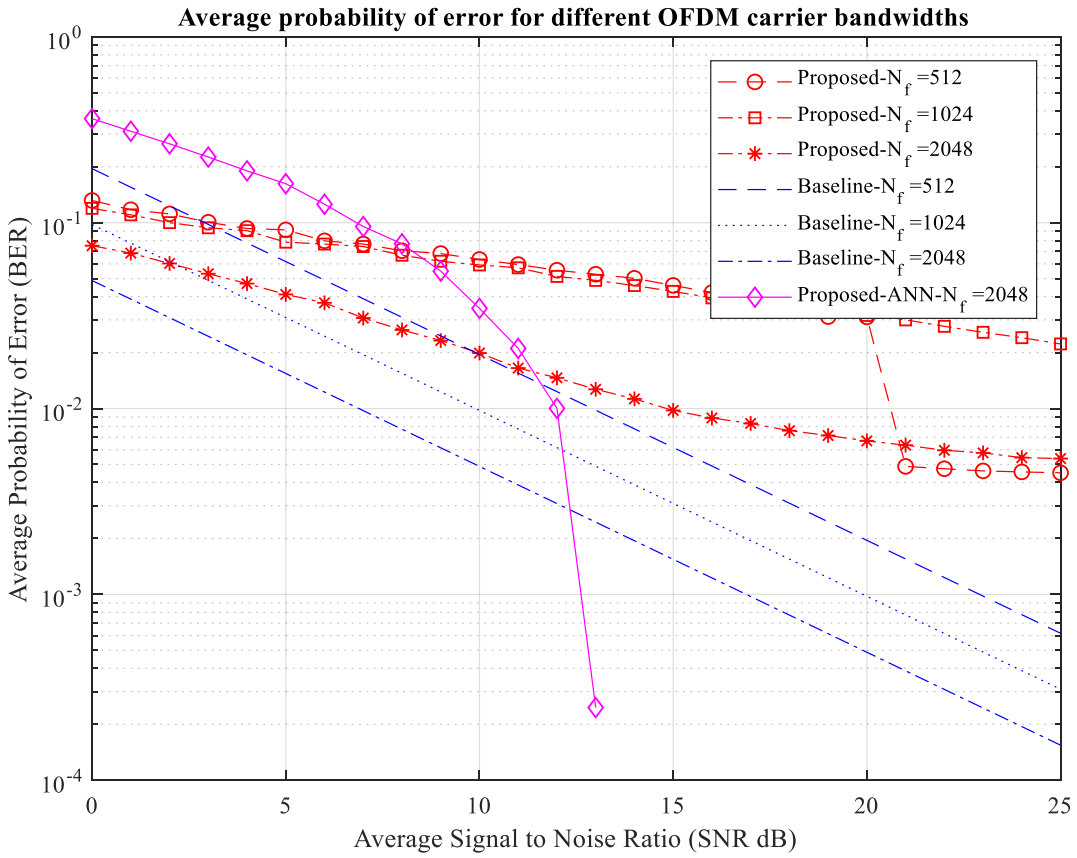

Figure 3: Maximum channel delay spread and average likelihood of error for various OFDM carrier bandwidths

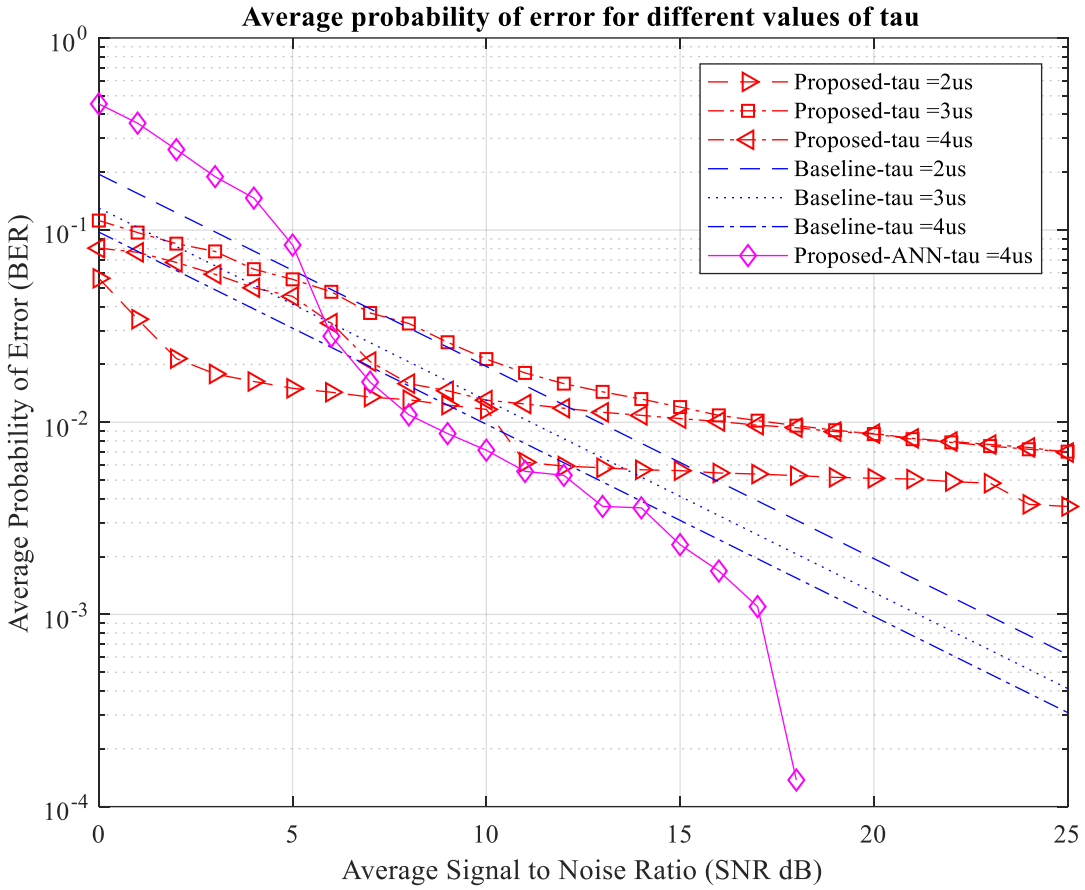

Figure 4: For various tau values, the average probability of mistake is calculated. The lines represent Monte-Carlo simulations, whereas the marks represent analytical formulations

At last, in Fig. 4, we change maximum channel delayspread,, and compare proposed scheme's likelihood of error to the baseline. According to the graph, proposed technique outperforms baseline for entire delay spread values. Furthermore, unlike[14], which depends on remaining portion of cyclic prefix and misses for high delay spread values, the suggested technique appears to be unaffected by changes in the delay spread. It's worth noting that the analytical likelihood of mistake matches the one determined by simulations, indicating that our methodology is correct.

7. CONCLUSION

Over ambient OFDM signals, we developed a unique technique for implementing binary frequency shift keying in backscatter systems. The suggested method uses a cycle of various phase shifts to provide unidirectional bandpass frequency shifts, allowing BFSK to be implemented over ambient OFDM signals. We avoided direct-link and adjacent channel interference by utilising guard band subcarriers and the orthogonality of the OFDM waveform. We also looked at the best noncoherent detector and came up with an exact expression for the average likelihood of error. Two limitations of energy detection-based approaches are avoided by the suggested scheme. For starters, it enables simple thresholdless detection and eliminates the need for the reader to estimate the SNR. Second, the error

probability for '1's and'0's are symmetric. Our simulation findings backed up our study, demonstrating that the suggested technique outperforms existing energy detection schemes by up to 3 dB.

REFERENCES

[1] V. Liu *et al.*, "Ambient backscatter: wireless communication out of thinair," in *Proc. of the ACM SIGCOMM Conf.*, Hong Kong, China, Aug.2013, pp. 39–50.
[2] A. N. Parks *et al.*, "Turbocharging ambient backscatter communication,"in *Proc. of the ACM SIGCOMM Conf.*,Chicago, IL, Aug. 2014, pp.619–630.
[3] B. Kellogg *et al.*, "Wi-fi backscatter: internet connectivity for RFpowered devices," in *Proc. of the ACMSIGCOMM Conf.*, Chicago,IL, Aug. 2014, pp. 607–618.
[4] D. Bharadia*et al.*, "BackFi: high throughput WiFi backscatter," in *Proc.of the ACM SIGCOMM Conf.*, London, U.K., Aug. 2015, pp. 283–296.
[5] P. Zhang *et al.*, "Enabling practical backscatter communication for onbody sensors," in *Proc. of the ACMSIGCOMM Conf.*, New York, NY,Aug. 2016, pp. 370–383.
[6] V. Iyer*et al.*, "Inter-technology backscatter: towards internet connectivity for implanted devices," in *Proc. of theACM SIGCOMM Conf.*,Florianopolis, Brazil, Aug. 2016, pp. 356–369.´
[7] A. Wang *et al.*, "FM backscatter: Enabling connected cities and smartfabrics," in *Proc. of the 14th USENIX Conf. on Netw. Syst. Des. AndImplementation*, Mar. 2017, pp. 243–258.
[8] Y. Peng*et al.*, "PLoRa: A passive long-range data network from ambientLoRa transmissions," in *Proc. of theACM SIGCOMM Conf.*, Aug. 2018,pp. 147–160.
[9] R. Duan*et al.*, "On the achievable rate of bi-static modulated re-scattersystems," *IEEE Trans. Veh. Technol.*, vol. 66, no. 10, pp. 9609–9613,Oct. 2017.
[10] G. Wang *et al.*, "Uplink detection and BER analysis for ambientbackscatter communication systems," in *Proc. IEEE Global Commun.Conf. (GLOBECOM)*, San Diego, CA, Dec. 2015.
[11] Z. Mat *et al.*, "Signal detection for ambient backscatter system withmultiple receiving antennas," in *Proc.IEEE 14th Canadian Workshopon Inform. Theory (CWIT)*, St. John's, NL, Canada, Jul. 2015, pp. 50–53.
[12] J. Qian*et al.*, "Noncoherent detections for ambient backscatter system,"*IEEE Trans. Wireless Commun.*, vol. 16, no. 3, pp. 1412–1422, Mar.2017.
[13] ——, "Semi-coherent detection and performance analysis for ambientbackscatter system," *IEEE Trans. Commun.*, vol. 65, no. 12, pp. 5266–5279, Dec. 2017.
[14] G. Yang and Y. C. Liang, "Backscatter communications over ambientOFDM signals: transceiver design and performance analysis," in *Proc.IEEE Global Commun. Conf. (GLOBECOM)*, Washington, DC, Dec.2016, pp. 1–6.
[15] M. A. ElMossallamy*et al.*, "Backscatter communications over ambientofdmsignals using null subcarriers," in *Proc. IEEE Global Commun.Conf. (GLOBECOM)*, Abu Dhabi, UAE, Dec. 2018, pp. 1–6.
[16] D. Darsena*et al.*, "Modeling and performance analysis of wirelessnetworks with ambient backscatter devices," *IEEE Trans. Commun.*,vol. 65, no. 4, pp. 1797–1814, Apr. 2017.

[17] F. Jameel, W. U. Khan, M. A. Jamshed, H. Pervaiz, Q. Abbasi, and R. Jäntti, “Reinforcement learning for scalable and reliable power allocation in sdn-based backscatter heterogeneous network,” in *Proc. IEEE INFOCOM Workshops*. IEEE, 2020, pp. 1069–1074.
[18] Matsuoka, H.; Doi, Y.; Yabe, T.; Sanada, Y., "Performance of overloaded MIMO-OFDM system with repetition code," in Intelligent Signal Processing and Communication Systems (ISPACS), 2014 International Symposium on , vol., no., pp.239-244, 1-4 Dec. 2014.
[19] Long Shi; Wei Zhang; Xiang-Gen Xia, "Space-Frequency Codes for MIMO-OFDM Systems with Partial Interference Cancellation Group Decoding," in Communications, IEEE Transactions on , vol.61, no.8, pp.3270-3280, August 2013.
[20] Doi, Y.; Inamori, M.; Sanada, Y., "Complexity reduction in joint decoding of block coded signals in overloaded MIMOOFDM system," in Intelligent Signal Processing and Communications Systems (ISPACS), 2013 International Symposium on , vol., no., pp.590-595, 12-15 Nov. 2013.
[21] M. A. ElMossallamy*et al.*, “Noncoherent backscattercommunications over ambient ofdm signals,” in *IEEE Trans. on Commun., to be published*. [Online]. Available:http://dx.doi.org/10.1109/TCOMM.2019.2899301
[22] Y. P. E. Wang *et al.*, “A primer on 3gpp narrowband internet of things,”*IEEE Communications Magazine*, vol. 55, no. 3, pp. 117–123, Mar.2017.
[23] A. Ghosh*et al.*, *Fundamentals of LTE*, 1st ed. Upper Saddle River,NJ: Prentice Hall Press, 2010.
[24] J. F. Ensworth and M. S. Reynolds, “Every smart phone is a backscatterreader: Modulated backscattercompatibility with bluetooth 4.0 lowenergy (BLE) devices,” in *IEEE Int. Conf. on RFID (RFID)*, San Diego,CA, Apr. 2015, pp. 78–85.
[25] J. Proakis and M. Salehi, *Digital Communications, 5th Edition*, 5th ed.McGraw-Hill Education, 2007.
[26] I. S. Ansari *et al.*, “On the sum of gamma random variates with application to the performance of maximal ratiocombining over nakagamim fading channels,” in *IEEE 13th Int. Workshop on Signal Process.Advances in Wireless Commun. (SPAWC)*, Cesme, Turkey, Jun. 2012,pp. 394–398.
[27] Wolfram Research Inc., *The Wolfram Functions Site*. [Online].Available: http://functions.wolfram.com
[28] McCulloch, Warren S., and Walter Pitts. "A logical calculus of the ideas immanent in nervous activity." *The bulletin of mathematical biophysics* 5, no. 4 (1943): 115-133.